

Two-Dimensional Simulation Model of Sediment Removal and Flow in Rectangular Sedimentation Basin

Gh. Naser¹; B. W. Karney²; and A. A. Salehi³

Abstract: A steady, two-dimensional numerical model was created to study the hydrodynamics of a rectangular sedimentation basin under turbulent conditions. The strip integral method was used to formulate the flow equations, using a forward marching scheme for solving the governing partial differential equations of continuity, momentum, advection–diffusion, turbulent kinetic energy, and its dissipation. In this way the flow equations were converted to a set of ordinary differential equations (ODEs) in terms of the key physical parameters. These parameters, along with a set of shape functions, describe flow variables including the velocity, the concentration of suspended sediments, and both the kinetic energy and its dissipation rate. Four Gaussian distributions were investigated, one corresponding to each flow parameter. In order to calculate the turbulent shear stresses, a two-equation turbulence model (i.e., k - ϵ model) was used. A fourth order Runge–Kutta method numerically integrates the set of ODEs. Simulation results were compared with experimental data, and close agreement (generally within 5–10%) was observed.

DOI: 10.1061/(ASCE)0733-9372(2005)131:12(1740)

CE Database subject headings: Sedimentation; Simulation models; Abatement and removal; Solids flow; Water treatment plants; Turbulence.

Introduction

Sedimentation, or settling by gravity, is a common method to separate water and solid particles in water and wastewater treatment plants as well as desilting basins. All attempts to model the sedimentation process must consider both the characteristics of the sediment and the fluid motion. In this way, the current study not only focuses on the hydrodynamics of the flow using a relatively efficient computer simulation model, but also improves the understanding of both flow and sediment characteristics. The fact that the profile of each flow parameter is to a significant degree self-similar forms the foundation of the simulation model by which the governing equations for flow are easily and quickly solved.

The relevant sediment characteristics are not only the settling velocities of the individual particles but also whether they retain their individualities as they settle. When two particles of a nonfloculent material come together, the only effect is the momentary mutual interference; if two particles of flocculent material interact they combine into a new particle with different properties. Thus, during the sedimentation of nonfloculent

materials the sediment characteristics are constant, while the characteristics of flocculent materials change continuously in a way that depends on both the sediment and flow characteristics. Mixing increases the chances of contact between the individual particles, and consequently the speed of coagulation; yet, the shear stresses between the particles set up by the velocity gradients also tend to limit the size to which these particles can grow. This study focuses primarily on the sedimentation of the nonfloculent materials whose settling velocity is described by Stokes law.

The relevant characteristics of fluid motion are not only the movement of the fluid as a whole but also the momentary fluctuations at every point in the fluid mass. To account for the bulk fluid motion, the boundaries of the flow, the average velocities, and their variations with time and space should be known or determined. In addition, all secondary motions such as convection or displacement currents and their fluctuations, which are the characteristics of turbulent flow, must also be defined or determined.

As settlement occurs, continuity requires that any upward current caused by localized secondary motion must be compensated by an equivalent downward flow. Since the fluid is progressively clearing with depth, the suspended matter tends to become more concentrated near the bottom. Hence, an upward flow carries fluid from a region of higher concentration into a relatively clear zone. Likewise, a downward current carries fluid with lower concentration into the region with higher concentration. Thus, one effect of secondary motion is to create a net upward transport, which tends to retard the rate at which the suspension clears. Conversely, the secondary motion may increase the rate of coagulation, which might increase the rate of sedimentation. Overall, whether a suspension of flocculent material will settle more rapidly in a turbulent fluid depends upon the relative increase in the rate of coagulation compared to upward transported rate. In a suspension of discrete particles, the upward transport is the only effect of

¹PhD Candidate, Civil Engineering Dept., Univ. of Toronto, Toronto, Ontario, Canada, M5S 1A4.

²Professor, Civil Engineering Dept., Univ. of Toronto, Toronto, Ontario, Canada, M5S 1A4 (corresponding author).

³Professor, Civil Engineering Dept., Tarbiat-Modares Univ. Tehran, Iran.

Note. Discussion open until May 1, 2006. Separate discussions must be submitted for individual papers. To extend the closing date by one month, a written request must be filed with the ASCE Managing Editor. The manuscript for this paper was submitted for review and possible publication on July 9, 2003; approved on February 3, 2005. This paper is part of the *Journal of Environmental Engineering*, Vol. 131, No. 12, December 1, 2005. ©ASCE, ISSN 0733-9372/2005/12-1740-1749/\$25.00.

turbulence and hence sedimentation is retarded. The complexities involved in the analysis of the secondary motions themselves, combined with those involved with coagulation, greatly complicate the sedimentation problems. However, an understanding of the separate effects of secondary motions and of coagulation on sedimentation would be helpful in understanding the entire phenomenon.

The current paper and its predecessors (Naser 1993 and Naser et al. 2002, 2003) describe a steady two-dimensional (2D) numerical model of the hydrodynamics of flow in a rectangular sedimentation basin (RSB) under turbulent conditions using the strip integral method (SIM). In this way, assuming fully developed flow and using Rajaratnam's velocity shape function, the flow equations were converted to a set of ordinary differential equations (ODEs) in terms of the key physical parameters. These parameters, along with a set of shape functions, describe variables such as the flow velocity, the concentration of suspended sediments, and both the kinetic energy and its dissipation rate. Four Gaussian distributions were studied, corresponding to each flow parameter. In order to calculate the turbulent shear stresses, the two-equation turbulence k - ϵ model was used. The classical fourth order Runge-Kutta method was used to integrate the set of ODEs. Finally, the numerical results of the model were compared with experimental data reported by others and show close agreement between the numerical and experimental results, thus generally demonstrating the validity of the numerical simulation.

The principal disadvantage of competing numerical approaches, such as finite element method and finite difference method (FDM), is that even for a simple 2D case they make large computational demands. Even by current standards, many earlier methods are computationally expensive. Therefore, particularly for the design purposes, a simpler but efficient method is desirable. In the current work, SIM is an attractive approach since it typically runs 1–2 orders of magnitude faster than many others (Abdel-Gawad and McCorquodale 1984).

Background

Hazen (1904) developed a theory for the settling particles in sedimentation basins. He made a distinction between quiescent and turbulent flow, and suspensions of discrete particles having a single settling velocity were analyzed. It was shown that the extent of the removal of discrete particles in a quiescent basin was independent of the depth. In an analytical/experimental study, Dobbins (1944) considered sedimentation of discrete particles of uniform size in a stream in which the turbulence was fully developed. He defined "fully developed turbulence" as a condition such that, although the velocity at every point was in a continuous state of flux, the key statistical properties remained constant. Dobbins verified the 1D model of turbulent sedimentation for discrete particle and provided the logarithmic law for the equilibrium vertical distribution of sediment within the basin.

Camp (1943) studied the case of sedimentation of discrete particles of varying settling velocities in a quiescent basin and then later presented a scheme to design primary sedimentation basins. On this basis, the performance of the sedimentation basin was thought to depend almost solely on the hydraulic detention time. Clements (1966) showed that the efficiency of the sedimentation basins was inversely proportional to the ratio of the flow depth to the depth of the inlet section. Using the "time-ratio" term (the ratio of effective flow-through time to effective settling time), Clements emphasized that the horizontal velocity varia-

tions across the breadth of RSBs strongly affected sedimentation efficiency, whereas the variations of velocity with depth have less effect on sedimentation if scouring is avoided. Not surprisingly, however, reality turned out to be more complex. In fact, more recent studies on sedimentation basins (McCorquodale 1976 and Larsen 1977) have revealed many ways in which the traditional detention-time view is inadequate. These studies have shown that the removal efficiency is affected by everything from density currents, turbulent mixing, inlet turbulence, free jet mixing, boundary layer growth, and flow recirculation.

Using the DuFort-Frankel method, Larsen (1977) not only solved the flow equations, but also carried out important experimental and field studies. This work helped to show the effects of turbulence and three-dimensional effects on the flow. Schamber and Larock (1978, 1981) focused on the numerical simulation of the flow, presenting a comprehensive finite element model to predict flow patterns in rectangular basins with surface inflow. They used a k - ϵ turbulence model along with five nonlinear algebraic equations for the Reynolds stresses and the turbulent energy flux correlation, thus creating 11 unknowns at each computational node, which were obtained using the Newton-Raphson approach. In their second paper (1981), they used a k - ϵ model with two transport equations for kinetic energy and dissipation and solved the resulting equations for five unknowns at each node.

Abdel-Gawad and McCorquodale (1984) developed a new numerical scheme, which simulated the flow in a rectangular basin as a nonstratified 2D turbulent but steady wall jet. Using a combination of SIM and FEM, they developed a numerical scheme to solve the Navier-Stokes equations. They used three shape functions for velocity, corresponding to the boundary layer, a potential core with free mixing, and a recirculation zone. The shape functions were a power law in the boundary layer, a uniform velocity distribution in the potential core, and followed a Gaussian distribution in the free mixing zone. They also used a modified mixing length approach to calculate turbulent shear stresses. Numerical results compared favorably with experimental velocity distributions and with field data.

Treating the sedimentation phenomenon as a diffusion process, Bechteler and Schrimf (1984, 1985) developed a numerical scheme to provide a better basis for dimensioning a horizontal sedimentation basin. To determine the turbulent eddy viscosity, they used Prandtl's theory for the turbulent mixing length and the logarithmic law for the distribution of velocity in open straight channels. Comparison between simulation and laboratory results demonstrated practical value of the model.

Lyn et al. (1992) studied several settling classes with different settling velocities in a 2D analytical model, thus showing that the influent settling velocity distribution was critical for accurately predicting of removal efficiencies. Then Zhou and McCorquodale (1992), and later Kerbs et al. (1996), applied the settling function of Takacs et al. (1991) to model the specific settling behavior of activated sludge. In their study, Zhou and McCorquodale (1992) analytically investigated the effects of density stratification on the hydrodynamics in the rectangular settling basins. They modeled the so-called density waterfall phenomenon at the front end of the basin. In these simulations, the sludge withdrawal took place homogeneously over the bottom boundary while the upper end of the sludge blanket was regarded as the lower boundary of the computational domain.

In 1999, Lakehal et al. (1999) studied analytically the hydrodynamics of flow (continuity, momentum, and advection-diffusion equations) in a circular, center-feed secondary clarifier with inclined bottom and central sludge withdrawal. Using a finite

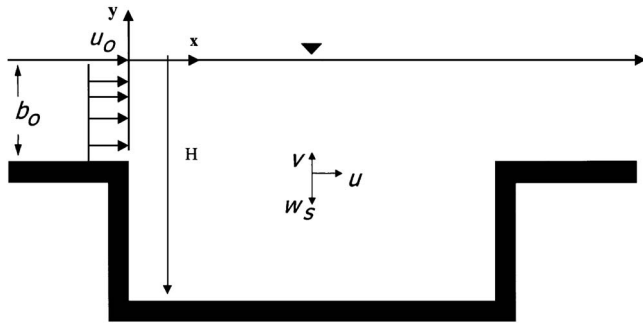


Fig. 1. Flow in sedimentation basin

volume approach and assuming axisymmetry properties for flow, they modeled flow and the settling processes in a radial section by using the $k-\varepsilon$ turbulence model on a 2D nonorthogonal grid. They investigated the sensitivity of flow to the rheological properties of sludge (including effective of sludge viscosity), settling characteristics of sludge, and the effects of stratification on the turbulent diffusion. The model results confirmed that the flow was strongly stratified with almost horizontal layers, and that the main flow developed along these stratified layers. The sensitivity analysis revealed that the overall picture of flow and concentration fields remained similar for all parameter variations.

Mathematical Model

The current research applied SIM to solve the hydrodynamics of turbulent jets in RSBs. The flow in the primary RSBs was modeled as a 2D turbulent surface jet. The flow was assumed to be steady in a time-averaged sense, nonstratified and incompressible. Therefore, the density was considered to be constant and equal to the density of clear water at the same temperature. In reality, although the flow depth decreases slightly with distance in a sedimentation basin, it was herein assumed constant. A more sophisticated model might eventually consider the effect of sedimentation process and the variations of depth on flow pattern. The idealized computational flow domain for the problem considered in the study is shown in Fig. 1 in which x and y are the horizontal and vertical Cartesian coordinate axes; u and v are the time-averaged velocity components in x and y directions; b_0 , u_0 , are the flow depth and the horizontal uniform velocity of flow at the inlet section; H is the water depth in the basin; and w_s is the falling velocity of solids, respectively.

Flow Equations

As Schlichting (2000) argued, the problems in free turbulent flow (including surface jets) are of a boundary layer nature; that is the region of space in which a solution is sought does not extend as far in a transverse direction as it does in the primary direction of flow, and thus the transverse gradients dominate. Considering this and applying the model assumptions to the general form of the Reynolds equations (Rodi 1980), the governing equations for 2D time-averaged steady turbulent surface jet (continuity, momentum, and transport advection diffusion equations) can be expressed as follows:

$$\frac{\partial u}{\partial x} + \frac{\partial v}{\partial y} = 0 \quad (1)$$

$$u \frac{\partial u}{\partial x} + v \frac{\partial u}{\partial y} = \frac{1}{\rho} \frac{\partial \tau}{\partial y} \quad (2)$$

$$u \frac{\partial C}{\partial x} + v \frac{\partial C}{\partial y} = \frac{\partial}{\partial y} \left(\Gamma \frac{\partial C}{\partial y} \right) + w_s \frac{\partial C}{\partial y} \quad (3)$$

In these equations, the parameters C, τ, Γ, ρ = concentration of suspended solids, turbulent shear stress, turbulent diffusion coefficient, and density of clear water, respectively. The current study was based on the assumption of primary sedimentation for suspended solids; that is the settlement of each solid constituent occurs independently. Hence, using Stokes law (Crowe et al. 2001), the settling velocity of the suspended solids, w_s , is considered known in the study.

Considering the Boussinesque assumptions, the turbulent shear stress is expressed as

$$\tau = -\overline{\rho u'v'} = \nu_t \partial u / \partial y \quad (4)$$

in which ν_t = turbulent eddy viscosity; u' and v' are the velocity fluctuations in x and y directions, respectively.

Turbulence Model

In order to calculate turbulent shear stress term in the Reynolds equation a two-equation turbulence model was used. The two-equation models reported in the literature often use the eddy-viscosity concept and the Kolmogorov–Prandtl expression for eddy viscosity (Rodi 1980). In the current study, the standard Jones–Launder $k-\varepsilon$ turbulence model was used to calculate shear stresses. This model is well established and has been used extensively in turbulent flow problems (Rodi 1980). Using the model assumptions, the transport equations for kinetic energy and its dissipation rate are as follows:

$$u \frac{\partial k}{\partial x} + v \frac{\partial k}{\partial y} = \frac{\partial}{\partial y} \left(\frac{\nu_t}{\sigma_k} \frac{\partial k}{\partial y} \right) + \nu_t \left(\frac{\partial u}{\partial y} \right)^2 - \varepsilon \quad (5)$$

$$u \frac{\partial \varepsilon}{\partial x} + v \frac{\partial \varepsilon}{\partial y} = \frac{\partial}{\partial y} \left(\frac{\nu_t}{\sigma_\varepsilon} \frac{\partial \varepsilon}{\partial y} \right) + C_{1\varepsilon} \frac{\varepsilon}{k} \nu_t \left(\frac{\partial u}{\partial y} \right)^2 - C_{2\varepsilon} \frac{\varepsilon^2}{k} \quad (6)$$

The turbulent eddy viscosity (ν_t) and turbulent diffusivity (Γ) are related through the Kolmogorov–Prandtl expression

$$\nu_t = C_\mu \frac{k^2}{\varepsilon} \quad (7)$$

and

$$\Gamma = \frac{\nu_t}{\sigma_t}$$

in which σ_t = Schmidt number. Typical values of the empirical coefficients σ_k , σ_ε , σ_t , C_μ , $C_{1\varepsilon}$, $C_{2\varepsilon}$ are 1.0, 1.3, 0.7, 0.09, 1.44, and 1.92, respectively (Rodi 1980).

Profiles/Shape Functions of Flow Parameters

The distribution of all flow parameters (i.e., velocity, concentration, kinetic energy, and its dissipation) in the sedimentation basins are based on reported experimental data. Townsend (1956) argued that the distribution of each flow parameter is similar at all

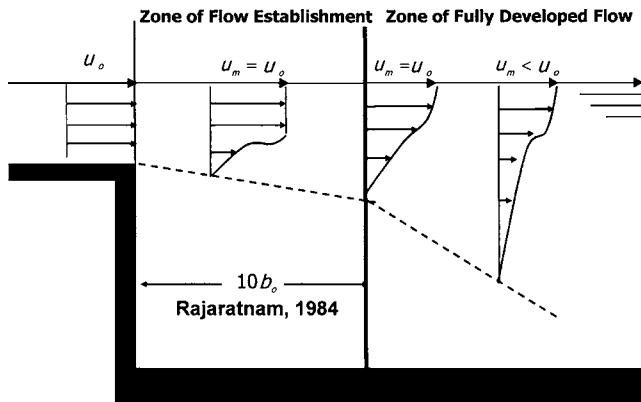


Fig. 2. Development of surface jet

cross sections of flow; consequently, the distribution of each flow parameter could be expressed in terms of a length scale and a corresponding scale of that flow parameter. More recently, Davidson and Pun (1999) showed that profiles of flow parameters are self-similar and are reasonably predicted by a Gaussian distribution.

Hence, using the Gaussian or normal distribution, a typical flow parameter, φ , may be expressed as follows:

$$\frac{\varphi}{\varphi_m} = \exp[\alpha_\varphi(\eta - \eta_\varphi)^2] \quad (8)$$

in which $\eta = y/b =$ dimensionless independent variable; $b =$ half width of the jet (some relevant length scale of the shear layer, which is defined here as the y coordinate of the point at which the velocity is half of the maximum velocity; or $u/u_m = 0.5$); $\varphi_m =$ maximum value of the flow parameter φ ; $\eta_\varphi =$ mean of the distribution or the dimensionless position of φ_m ; and α_φ sets the spread of the distribution around its mean.

The development of the surface jet and related flow patterns in the sedimentation basin are shown in Fig. 2. As this figure makes clear, different patterns of flow occur in the developing zone and the fully developed zone. The velocity profile at the inlet section is idealized as uniform throughout the section, at all points equal to its initial value, u_0 . However, the velocity in the developing zone is equal to u_0 in some places and less than u_0 at others. This velocity decreases in the flow direction until, at the distance $L = 10b_0$ (Rajaratnam, 1976; Rajaratnam and Humphries 1984), only the velocity at the free surface is still u_0 . However, in the second zone the velocity at all points of flow domain (even at the free surface) is less than initial velocity in the inlet section, u_0 . The flow in this zone is termed fully developed.

Interestingly, the shape function is simple for the case of the velocity distribution. In fact, the velocity distribution in the settling basins is assumed to be similar to that observed experimentally in plane jets. Since the maximum velocity is almost always at the free surface, the value of η_u for velocity in Eq. (8) is set to zero. On the other hand, using the experimental measurements on turbulent surface jets by Rajaratnam (1976 and Rajaratnam and Humphries 1984), the mean x component velocity distribution for fully developed flow in the settling basin can be expressed as

$$u = u_\infty + u_m \exp(-0.693\eta^2) \quad (9a)$$

Although Rajaratnam (1965) argued that the contribution of reverse flow to the momentum balance would be relatively small, the term u_∞ is introduced to permit the effect of the reverse

velocity at the bottom of the basin on the settling of the solids.

For the concentration of suspended solid particles, kinetic energy and its dissipation (i.e., C, k, ε) the shape functions are similarly expressed as follows:

$$\frac{C}{C_m} = \exp[\alpha_c(\eta - \eta_c)^2] \quad (9b)$$

$$\frac{k}{k_m} = \exp[\alpha_k(\eta - \eta_k)^2] \quad (9c)$$

$$\frac{\varepsilon}{\varepsilon_m} = \exp[\alpha_\varepsilon(\eta - \eta_\varepsilon)^2] \quad (9d)$$

Numerical Solution of Governing Equations

A numerical model should not only be consistent, stable, and convergent to an accurate solution but it should also have desirable human attributes. It should be easy to use, easy to modify, easy to implement, and efficient in terms of computational time and memory requirements (Abbott and Minns 1998). An efficient scheme is the one that limits the computer processing time and memory usage. Even though the memory requirements have become less stringent, a less demanding technique can still solve larger problems.

Among the available numerical schemes, SIM has often been considered as one of the most suitable techniques for boundary layer or shear layer types of flow in open channels. Moses (1968) used SIM to analyze a boundary layer flow problem, approximating the velocity profile by polynomials and relating the shear stresses to average velocity. Narayanan (1972) used SIM to predict flow behavior downstream of a leaf gate and thereby developed a theoretical method to predict mean flow of a turbulent jet expanding in a duct of constant width. Using a power law for the velocity distribution, McCorquodale and Khalifa (1983) presented an analytical discussion of the hydraulic jump that solved the appropriate flow equations using SIM.

Strip Integral Method

The SIM is essentially a forward marching scheme in which the partial differential equations of flow are reduced to a set of ODEs in terms of the key flow parameters. This technique can only be applied to parabolic differential equations for which the primary flow direction is longitudinal and boundary layer assumptions are valid. However, the most important feature of SIM is its computational efficiency both in time and storage. According to both Abdel-Gawad and McCorquodale (1984) and Imam (1981), a complete simulation of a tank that has a depth/length ratio 1:7 will run SIM 12–15 times faster than a typical finite difference solution. The SIM is well noted for its numerical efficiency, computational accuracy, and programming simplicity (Abdel-Gawad and McCorquodale 1984).

In the current study, three unknown flow parameters; u_∞, u_m, b , and the other unknowns corresponding to the concentration, kinetic energy, and its dissipation were determined for each strip. The SIM, then, integrates the flow equations over appropriate “strips.” Subsequently, a set of ODEs must be solved for each corresponding unknown parameters of flow. In particular, the integral form of the continuity equation over y strips is

$$\int_y \frac{\partial u}{\partial x} dy + \int_y \frac{\partial v}{\partial y} dy = 0 \quad (10)$$

Substituting the shape functions for the horizontal component of velocity, u , from Eq. (9a) and changing the integral variable from y to η , the vertical component of velocity, v , is obtained in terms of the parameters of u 's shape function. The details are given in the Appendix.

Similarly, substituting the velocity, concentration, kinetic energy, and its dissipation from the set of Eq. (9a)–(9d) into Eqs. (2)–(6) and integrating over appropriate strips, the following integral forms of the flow equations are obtained as a set of ODEs:

$$cu_0 \frac{du_\infty}{dx} + cu_1 \frac{db}{dx} + cu_2 \frac{du_m}{dx} = cu_3 \quad (11a)$$

$$cc_0 \frac{du_\infty}{dx} + cc_1 \frac{db}{dx} + cc_2 \frac{du_m}{dx} + cc_3 \frac{dC_m}{dx} + cc_4 \frac{d\eta_c}{dx} + cc_5 \frac{d\alpha_c}{dx} = cc_6 \quad (11b)$$

$$ck_0 \frac{du_\infty}{dx} + ck_1 \frac{db}{dx} + ck_2 \frac{du_m}{dx} + ck_3 \frac{dk_m}{dx} + ck_4 \frac{d\eta_k}{dx} + ck_5 \frac{d\alpha_k}{dx} = ck_6 \quad (11c)$$

$$c\epsilon_0 \frac{du_\infty}{dx} + c\epsilon_1 \frac{db}{dx} + c\epsilon_2 \frac{du_m}{dx} + c\epsilon_3 \frac{d\epsilon_m}{dx} + c\epsilon_4 \frac{d\eta_\epsilon}{dx} + c\epsilon_5 \frac{d\alpha_\epsilon}{dx} = c\epsilon_6 \quad (11d)$$

in which all coefficients are given in the Appendix. Eqs. (11a)–(11d) are the integral forms of Reynolds/momentum equation, the advection–diffusion equation, the kinetic energy equation, and the transport equation for dissipation of kinetic energy, respectively.

Overall, the above system of equations involves 12 unknowns. Therefore, to solve this system mathematically the original flow equations must be integrated over three different strips. In fact, any independent combination of strips can be used. However, since the shear stress at the free surface is always zero, it is helpful to choose the free surface as lower limit of each strip. In this work, the first strip was taken from free surface to the half-width position (the interval $[0, b]$). It is convenient to take the whole depth of the basin (the interval $[0, H]$) for the second strip. For reasons related to the consistency and uniqueness of the solutions, the third strip could be any strip except the first two and the strip from half-width to the bottom of the basin (the interval $[b, H]$). In this work, $[0, b/2]$ was taken as the third strip. Integrating over these three strips, Eq. (11) can be expressed in matrix form as

$$\frac{d\mathbf{F}}{dx} = \mathbf{A}^{-1}\mathbf{B} \quad (12)$$

in which $\mathbf{F}=12 \times 1$ unknown matrix; $\mathbf{A}=12 \times 12$ coefficient matrix; and $\mathbf{B}=12 \times 1$ known vector. Using Eq. (11), the matrix \mathbf{F} is defined as follows:

$$\mathbf{F} = [u_\infty, b, u_m, C_m, \alpha_c, \eta_c, k_m, \alpha_k, \eta_k, \epsilon_m, \alpha_\epsilon, \eta_\epsilon]^T \quad (13)$$

and also the matrices \mathbf{A} and \mathbf{B} are obtained from the coefficients of Eq. (11). As detailed in the Appendix, these matrices are expressed in terms of the parameters of the four shape functions for velocity, concentration, kinetic energy, and its dissipation.

Inlet Boundary Conditions

The input parameters and boundary conditions for calculating sediment transport are seldom known exactly. Thus, the effects of these variations should be considered thoroughly. As is the case for any set of differential equations, boundary conditions are necessary to solve the system of equations given by Eq. (12). According to Rajaratnam (1976) and Rajaratnam and Humphries (1984), an appropriate initial value for the maximum velocity of the surface jet is

$$u_{m_0} = u_0 \quad (14)$$

and for the half width of the jet is

$$b = 0.7b_0 \quad (15)$$

According to Eq. (9b), the shape function of concentration was expressed in terms of three parameters, namely the maximum concentration and its position, and the coefficient α_c . Considering the uniform concentration C_0 at the inlet section, the position of the maximum concentration was assumed to be at the bottom of inlet section (or $\eta_{c_0} = b_0/0.7b_0 \approx 1.429$). Hence, setting $C_{m_0} = C_0$ the parameter α_c was calculated by equating the total initial concentration at the inflow section (due to uniform concentration profile) to the total concentration from Eq. (9b). Thus

$$\int C_0 dy = \int C dy = \int b C_m \exp[\alpha_c(\eta - \eta_c)^2] d\eta \quad (16)$$

Using Bradbory (1965) and Rodi (1980), the initial values for maximum kinetic energy and its dissipation may be expressed as follows:

$$k_{m_0} = 0.1u_0^2 \quad (17)$$

$$\epsilon_{m_0} = C_D \frac{k_{m_0}^{3/2}}{L_m}$$

in which L_m = turbulent mixing length, which for the case of a turbulent surface jet was approximated to $0.27b$.

According to the study by Nezu and Nakagawa (1993), in open channel flows the coefficient C_D is a strong function of the Reynolds number and the Kolmogorov constant. In other words, as the Reynolds number increases, the coefficient C_D decreases rapidly. However, for the fully turbulent flows (with very large Reynolds number) the coefficient approaches a constant value of the order of unity depending on the Kolmogorov constant. Details are given in Fig. 2.4 on page 22 of Nezu and Nakagawa (1993).

Using the same procedure as that for the concentration shape function, the initial values for other parameters; $a_k, a_\epsilon, \eta_k, \eta_\epsilon$, in the kinetic energy and dissipation shape functions were estimated.

Numerical Integration

Considering the inlet boundary conditions, the matrix expression in Eq. (12) must be solved for the unknown parameters of the shape functions and consequently for the corresponding unknown flow parameters. In this study, the classical fourth order Runge–Kutta method (Chapra and Canale, 2002) with a step size of $\Delta x/b_0 = 0.001$ was used to numerically integrate Eq. (12). The proposed model was used to predict the flow pattern for a surface jet and the concentration of suspended solids in a RSB. The details of the properties of the surface jet are given in Rajaratnam and Humphries (1984), and for the RSB in Bechteler and Schimpf (1984, 1985).

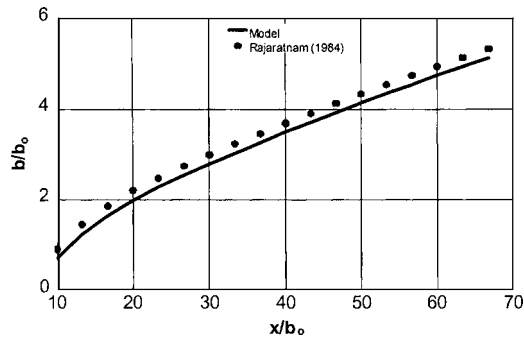


Fig. 3. Half width of jet

Analysis and Discussion of Numerical Modeling Results

Fig. 3 shows variations over the half width of the jet in the flow direction based on the model results and experimental data by Rajaratnam and Humphries (1984). As is clear, the excellent agreement between model and experiment attests to the accuracy of the SIM. Specifically, both model and experiment show a linear variation for the half width with a slope of 0.073 and 0.072 based on the model and experimental results, respectively. This agreement not only shows the general validity of the flow parameter shape functions—especially for the velocity and turbulent parameters—but also at least partially validates the turbulence model.

Fig. 4 compares the results of model for the maximum velocity in the computational flow domain with experimental data reported by Rajaratnam and Humphries (1984). The good agreement between model and experiment is again obvious. Clearly, variations may be divided into two different parts. Initially, ($x/b_0 \leq 30$), the velocity variations are sharp, but these changes gradually fade with distance and eventually approach a horizontal line. In this case, the flow achieves a steady uniform condition. Using nonlinear regression analysis, the following equation was deduced from the model results:

$$\frac{u_m}{u_{m0}} = \frac{\alpha}{(x/b_0)^\beta} \quad (18)$$

in which the estimated values of the parameters α and β are 3.1135 and 0.55, respectively. Rajaratnam and Humphries (1984) suggested the values 3.15 and 0.5 for the parameters α and β , respectively. The close agreement between estimated and

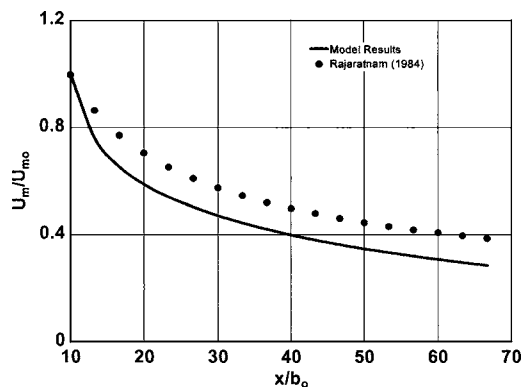


Fig. 4. Variations of maximum velocity in sedimentation basin

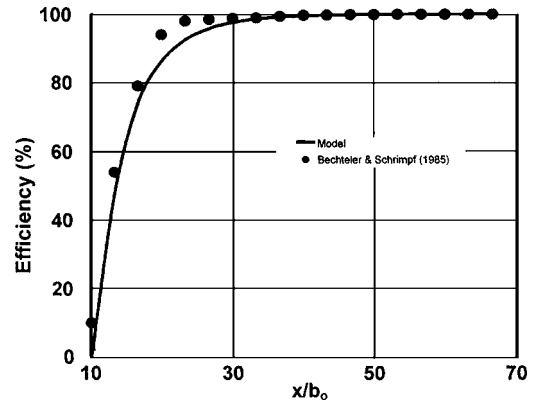


Fig. 5. Removal efficiency of sedimentation basin

suggested values for these parameters again supports the validity of the numerical model.

The efficiency of the basin is plotted with distance in Fig. 5, which also shows the experimental data published by Bechteler and Schrimpf (1985). The numerical results show that no material settles at the origin, an observation that supports the assumption of fully developed flow. However, around 10% of the experimental suspended loads do settle in the developing zone, thus indicating some error. Interestingly, however, the figure shows that at a distance farther from the inlet zone (i.e., $x/b_0 > 30$) the discrepancies all but disappear. Overall, the model predictions are reasonable, even though its assumptions are quite approximate.

Plots of the maximum kinetic energy and its dissipation are given in Fig. 6. The kinetic energy clearly decreases in the flow indicating a change in the flow from turbulent to steady uniform. Unfortunately, because of the difficulties of obtaining experimental data, the results of the turbulence part of the model cannot be directly compared with the experimental data. However, the accuracy of the velocity and removal efficiency approximately close indirectly support the performance of the proposed numerical model.

Fig. 7 shows the variations of absolute value of η_k and η_e along the basin. Satisfyingly, the maximum kinetic energy and maximum dissipation occur almost at the same position. This fact may again highlight the assumption of the equality of the production of kinetic energy and its dissipation in the k - ϵ turbulence model. Since the turbulence model forms a basis for calculating the coefficient C_μ , the model itself is thus partially validated.

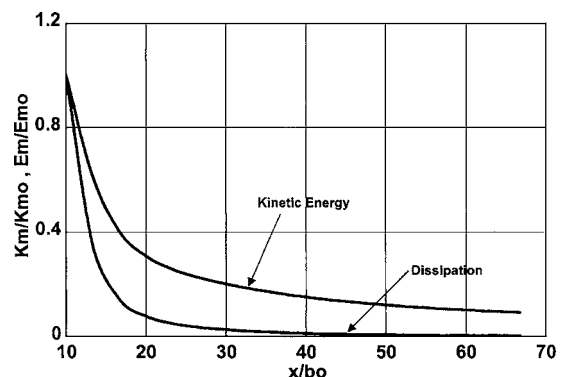


Fig. 6. Maximum kinetic energy and maximum dissipation

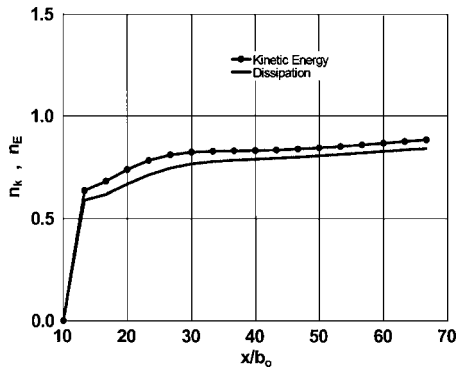


Fig. 7. Positions of maximum kinetic energy and maximum dissipation

Using Eq. (17) as initial values for kinetic energy and dissipation rate, a sensitivity analysis is conducted to investigate the importance of these parameters. Comparing with Bechteler and Schimpf (1985), the results of the analysis are given in Figs. 8 and 9, respectively. The general relations $k_m = a_1 u_m^2 / 2$ and $\epsilon_m = a_2 k_m^{3/2}$ are used to conduct the analysis. As is clear from the figures, the numerical results more strongly depend on the initial value of the dissipation term than they do on the kinetic energy term.

To study the effect of the inlet zone on the sedimentation process, a sensitivity analysis is performed on the so-called “aspect ratio” of the basin, defined by b_0/H , which H is the total depth of the basin. The ratio changes from 0.07 (for a small jet) to 0.96 (for nearly smooth open channel). Compared with Bechteler and Schimpf (1985), Fig. 10 shows the results of the analysis, indicating that the model efficiency is strongly affected by the basin’s aspect ratio. This result highlights the importance of the velocity shape function for the developing flow zone.

Practical Implications

The numerical model presented here was calibrated using the published experimental data and comparisons generally confirmed the validity of the numerical simulation under the model assumptions. In general, the results of the study for velocity and efficiency of the basin could be used in the design of the sedimentation basins. However, it must be born in mind that the effects of inlet and outlet zones on the removal efficiency of the basins were ignored in the current study, and this might have some bearings for the detailed design. Thus, ideally, a more robust and careful analysis might ultimately be necessary to address these limitations.

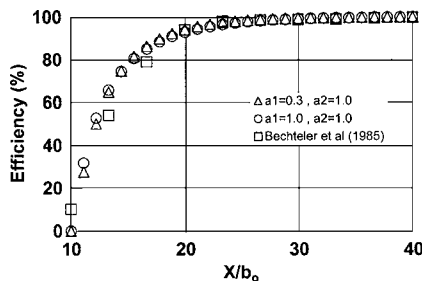


Fig. 8. Sensitivity analysis on initial value for kinetic energy

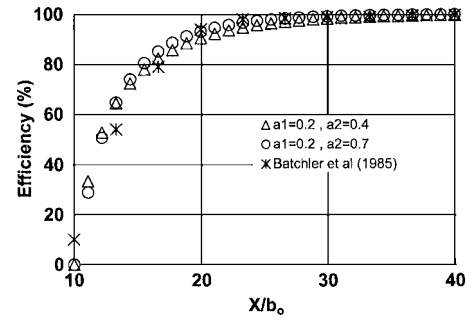


Fig. 9. Sensitivity analysis on initial value for dissipation rate

Treatment of Inlet Zone

Having considered the fully developed flow assumption, the effects of the inlet zone on the flow behavior were not thoroughly investigated in this study. Physically, the aspect ratio of the basin has a strong influence on the reverse flow and hence on the flow pattern. Although the fully developed flow assumption might be limiting, there was still reasonable agreement between the reported experimental data and the model’s results. The limitation of fully developed flow could be easily relaxed by using a more realistic velocity shape function, one that predicts the velocity variations in both the developing-flow and fully developed-flow zones. In fact, the velocity shape function in the first zone (developing-flow zone) should likely be expressed by two different formulas. The first formula demonstrates the uniform flow velocity at the potential core of the jet with depth δ (unknown parameter with maximum b_0 at inlet section and minimum zero at $x = 10 b_0$), which is equal to the initial velocity u_0 . The second formula could be the general form of Gaussian distribution Eq. (8) with the appropriate term representing the inverse flow. Then, the parameter δ and the shape function’s parameters would be determined through the simulation model at each cross section of the flow. For the second zone (fully developed-flow zone), Eq. (9a) remains valid.

Treatment of Withdrawal/Outlet Zone

The second limitation of the current model comes from the intrinsic nature of SIM, which is a forward marching numerical scheme that cannot be applied near the effluent weir (or outlet zone). Hence, a combination of SIM and FEM or FDM (for the outlet zone) is required to analyze the whole computational flow domain.

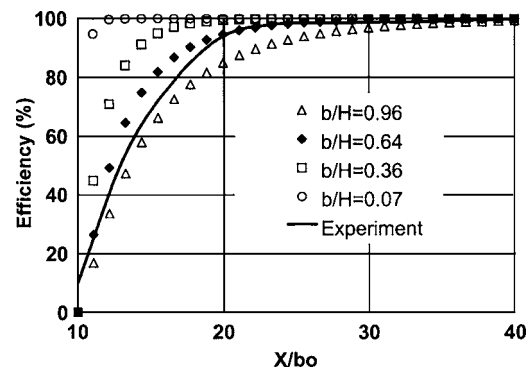


Fig. 10. Inlet zone effect on sedimentation process

Specification of Flow Field

In the current study, the specification of the flow as a surface jet might cause some practical limitations. In fact, the designers usually seek to avoid surface jets, since they lead to short-circuiting and recirculating flow patterns. If the flow pattern was taken as a wall jet, the simulation model might better apply to certain practical cases. Splitting the flow at each section into two layers, the wall-jet problem can also be solved using the SIM. In this case, the velocity shape function can be easily modified using a combination of the power law for the inner layer (close to the basin's bottom) and the Gaussian distribution for the outer layer (between the inner layer and free surface).

Treatment of Settling Velocity

The current study was based on the assumption of primary sedimentation for suspended solids. In other words, the settlement of each suspended solid was studied individually, and Stokes law was used to calculate the settling velocity of each particle. The process of coagulation and also the density-current phenomenon, particularly important in the secondary sedimentation basins used in the sewage treatment plants, might influence the settling of particles. In this case, due to coagulation of the solids, not only the settling velocity but also the local fluid density is no longer constant throughout the settling processes, but now depends upon the suspended solid's concentration. However, the current simulation model could easily be modified for these cases. What are needed are the local state equations relating a solid's concentration to its settling velocity and also to the density of water. A large number of empirical formulas have been proposed in the literature to describe these kinds of relationships (e.g., Takacs et al. 1991).

Conclusion

The current study not only focused on the hydrodynamic of flow in RSBs through a relatively efficient computer simulation model but also provided greater understanding of both flow and sediment characteristics. The fact that the profile of each flow parameter is approximately self similar made the critical base for the simulation model by which the governing equations for flow were easily solved. In this way, the strip integral method was applied to a typical RSB in order to simulate the flow pattern and dispersion characteristics. This method assumed a dominant flow direction and used shape functions for velocity and other flow parameters to reduce the flow equations to a set of simultaneous ODEs, which were solved readily by the classical fourth order Runge–Kutta method. The resulting method was easy to use, to modify, and to implement in a way that controls the numerical accuracy and convergence; these characteristics made SIM an efficient and practical approach especially for shear-layer flows.

The mathematical model satisfactorily predicted the internal mean flow structure for settling basins. The model showed also that the results were sensitive to the intensity of turbulent shear stress, but that the $k-\varepsilon$ turbulence model gave reasonable results. The model successfully predicted the velocity distribution, the concentration of the suspended load, and both the kinetic energy and its dissipation rate. Although the model results showed initially some error near the inlet section, the overall accuracy of the predicted removal efficiency by the computer simulation model confirmed the general validity of the model.

Appendix

The elements of the coefficient matrix **A** and the vector **B** in Eq. (12) as derived from Eqs. (1)–(6) are as follows (the indices i and j refer to lower and upper limit of each strip, respectively):

Continuity Equation

Replacing the shape function for the horizontal velocity component from Eq. (9a) into the continuity Eq. (1), and then integrating the equation over y , the vertical velocity component of flow, v , is obtained as

$$v_j = v_i - [b(\eta_j - \eta_i)] \frac{du_\infty}{dx} - (bI_u^1) \frac{du_m}{dx} + u_m[(\eta_j f_{u_j} - \eta_i f_{u_i}) - I_u^1] \frac{db}{dx} \quad (19)$$

Coefficients in Momentum Equation

Using Eqs. (9a) and (19) for velocity components and integrating momentum Eq. (2) over y , the elements of the coefficient matrix **A** and the vector **B** corresponding to the momentum equation are evaluated as

$$Cu_0 = b[(u_\infty - u_m f_{u_j})(\eta_j - \eta_i) + 2u_m I_u^1] \quad (20)$$

$$Cu_1 = u_m[u_\infty(\eta_i f_{u_i} - \eta_j f_{u_j} + I_u^1) + u_m \eta_i f_{u_i}(f_{u_i} - f_{u_j}) + u_m(I_u^2 - f_{u_j} I_u^1)] \quad (21)$$

$$Cu_2 = b[(u_\infty - u_m f_{u_j}) I_u^1 + 2u_m I_u^2] \quad (22)$$

$$Cu_3 = u_m[(v_{t_j} f'_{u_j} - v_{t_i} f'_{u_i})/(\rho b) + v_i(f_{u_i} - f_{u_j})] \quad (23)$$

$$I_u^1 = \int_{\eta_i}^{\eta_j} f_u d\eta = \frac{C}{\sqrt{0.693}} [\text{erf}(\sqrt{0.693}\eta_j) - \text{erf}(\sqrt{0.693}\eta_i)] \quad (24)$$

$$I_u^2 = \int_{\eta_i}^{\eta_j} f_u^2 d\eta = \frac{C}{\sqrt{2 \times 0.693}} [\text{erf}(\sqrt{2 \times 0.693}\eta_j) - \text{erf}(\sqrt{2 \times 0.693}\eta_i)] \quad (25)$$

in which $\text{erf}(z)$ = mathematical error function and C = constant equal to $\sqrt{\pi}/2$.

Coefficients in Turbulence Model Equations

Equation of Kinetic Energy

Using the previously defined shape functions for velocity components, kinetic energy and its dissipation and integrating the transport equation for kinetic energy Eq. (5) over y , the following relations are obtained for the coefficients in matrices **A** and **B** in Eq. (12) corresponding to the kinetic energy equation:

$$C_{K0} = bk_m I_K^1 - bk_m f_{Kj} (\eta_j - \eta_i) \quad (26)$$

$$C_{K1} = -u_\infty k_m [(\eta_j f_{Kj} - \eta_i f_{Ki}) - I_K^1] - u_m k_m I_K^3 - u_m k_m [(\eta_j f_{Uj} f_{Kj} - \eta_i f_{Ui} f_{Ki}) - I_K^2 - I_K^3] + u_m k_m f_{Kj} (\eta_j f_{Uj} - \eta_i f_{Ui}) - u_m k_m f_{Kj} I_U^1 \quad (27)$$

$$C_{K2} = bk_m I_K^2 - bk_m f_{Kj} I_U^1 \quad (28)$$

$$C_{K3} = bu_\infty I_K^1 + bu_m I_K^2 \quad (29)$$

$$C_{K4} = -bu_\infty k_m (f_{Kj} - f_{Ki}) - bk_m u_m [(f_{Uj} f_{Kj} - f_{Ui} f_{Ki}) - I_K^4] \quad (30)$$

$$C_{K5} = [bu_\infty k_m / (2a_K)] \{[(\eta_j - \eta_K) f_{Kj} - (\eta_i - \eta_K) f_{Ki}] - I_K^1\} + [bu_m k_m / (2a_K)] \{[(\eta_j - \eta_K) f_{Uj} f_{Kj} - (\eta_i - \eta_K) f_{Ui} f_{Ki}] - I_K^2 - I_K^3 + \eta_K I_K^4\} \quad (31)$$

$$C_{K6} = k_m v_i (f_{Ki} - f_{Kj}) + \left(\frac{k_m}{b\sigma_K}\right) (v_{ij} f'_{Kj} - v_{ii} f'_{Ki}) + \left(\frac{u_m^2}{b}\right) I_K^5 - b\varepsilon_m I_\varepsilon^1 \quad (32)$$

$$I_K^1 = \int_{\eta_i}^{\eta_j} f_K d\eta \quad (33)$$

$$I_K^2 = \int_{\eta_i}^{\eta_j} f_U f_K d\eta \quad (34)$$

$$I_K^3 = \int_{\eta_i}^{\eta_j} \eta f'_U f_K d\eta \quad (35)$$

$$I_K^4 = \int_{\eta_i}^{\eta_j} f'_U f_K d\eta \quad (36)$$

$$I_K^5 = \int_{\eta_i}^{\eta_j} v_i (f'_K)^2 d\eta \quad (37)$$

Equation of Dissipation

Using the previously defined shape functions for velocity components, kinetic energy and its dissipation and integrating the transport equation for dissipation term Eq. (6) over y , the following relations are obtained for the coefficients in matrices **A** and **B** in Eq. (12) corresponding to the ε equation:

$$C_{\varepsilon 0} = b\varepsilon_m I_\varepsilon^1 - b\varepsilon_m f_{\varepsilon j} (\eta_j - \eta_i) \quad (38)$$

$$C_{\varepsilon 1} = -u_\infty \varepsilon_m [(\eta_j f_{\varepsilon j} - \eta_i f_{\varepsilon i}) - I_\varepsilon^1] - u_m \varepsilon_m I_\varepsilon^3 - u_m \varepsilon_m [(\eta_j f_{Uj} f_{\varepsilon j} - \eta_i f_{Ui} f_{\varepsilon i}) - I_\varepsilon^2 - I_\varepsilon^3] + u_m \varepsilon_m f_{\varepsilon j} (\eta_j f_{Uj} - \eta_i f_{Ui}) - u_m \varepsilon_m f_{\varepsilon j} I_U^1 \quad (39)$$

$$C_{\varepsilon 2} = b\varepsilon_m I_\varepsilon^2 - b\varepsilon_m f_{\varepsilon j} I_U^1 \quad (40)$$

$$C_{\varepsilon 3} = bu_\infty I_\varepsilon^1 + bu_m I_\varepsilon^2 \quad (41)$$

$$C_{\varepsilon 4} = -bu_\infty \varepsilon_m (f_{\varepsilon j} - f_{\varepsilon i}) - b\varepsilon_m u_m [(f_{Uj} f_{\varepsilon j} - f_{Ui} f_{\varepsilon i}) - I_\varepsilon^4] \quad (42)$$

$$C_{\varepsilon 5} = [bu_\infty \varepsilon_m / (2a_\varepsilon)] \{[(\eta_j - \eta_\varepsilon) f_{\varepsilon j} - (\eta_i - \eta_\varepsilon) f_{\varepsilon i}] - I_\varepsilon^1\} + [bu_m \varepsilon_m / (2a_\varepsilon)] \{[(\eta_j - \eta_\varepsilon) f_{Uj} f_{\varepsilon j} - (\eta_i - \eta_\varepsilon) f_{Ui} f_{\varepsilon i}] - I_\varepsilon^2 - I_\varepsilon^3 + \eta_\varepsilon I_\varepsilon^4\} \quad (43)$$

$$C_{\varepsilon 6} = \varepsilon_m v_i (f_{\varepsilon i} - f_{\varepsilon j}) + \left(\frac{\varepsilon_m}{b\sigma_\varepsilon}\right) (v_{ij} f'_{\varepsilon j} - v_{ii} f'_{\varepsilon i}) + \left(C_{1\varepsilon} C_\mu \frac{k_m u_m^2}{b}\right) I_\varepsilon^5 - C_{2\varepsilon} \frac{b\varepsilon_m^2}{k_m} I_{K\varepsilon} \quad (44)$$

$$I_\varepsilon^1 = \int_{\eta_i}^{\eta_j} f_\varepsilon d\eta \quad (45)$$

$$I_\varepsilon^2 = \int_{\eta_i}^{\eta_j} f_U f_\varepsilon d\eta \quad (46)$$

$$I_\varepsilon^3 = \int_{\eta_i}^{\eta_j} \eta f'_U f_\varepsilon d\eta \quad (47)$$

$$I_\varepsilon^4 = \int_{\eta_i}^{\eta_j} f'_U f_\varepsilon \varepsilon d\eta \quad (48)$$

$$I_\varepsilon^5 = \int_{\eta_i}^{\eta_j} (f'_U)^2 f_K \varepsilon d\eta \quad (49)$$

$$I_{K\varepsilon} = \int_{\eta_i}^{\eta_j} \frac{f_\varepsilon^2}{f_K} d\eta \quad (50)$$

Advection-Diffusion Equation

Using the previously defined shape functions for velocity components, concentration, kinetic energy and its dissipation and integrating Eq. (3) over y , the following relations are obtained for the coefficients in matrices **A** and **B** in Eq. (12) corresponding to the advection-diffusion equation:

$$C_{c0} = bC_m I_c^1 - bC_m f_{cj} (\eta_j - \eta_i) \quad (51)$$

$$C_{c1} = -U_\infty C_m [(\eta_j f_{cj} - \eta_i f_{ci}) - I_c^1] - u_m C_m I_c^3 - u_m C_m [(\eta_j f_{Uj} f_{cj} - \eta_i f_{Ui} f_{ci}) - I_c^2 - I_c^3] + u_m C_m f_{cj} (\eta_j f_{Uj} - \eta_i f_{Ui}) - u_m C_m f_{cj} I_U^1 \quad (52)$$

$$C_{c2} = bC_m I_c^2 - bC_m f_{cj} I_U^1 \quad (53)$$

$$C_{c3} = bu_\infty I_c^1 + bu_m I_c^2 \quad (54)$$

$$C_{c4} = -bu_\infty C_m (f_{cj} - f_{ci}) - bC_m u_m [(f_{Uj} f_{cj} - f_{Ui} f_{ci}) - I_c^4] \quad (55)$$

$$C_{c5} = [bu_\infty C_m / (2a_c)] \{[(\eta_j - \eta_c) f_{cj} - (\eta_i - \eta_c) f_{ci}] - I_c^1\} + [bu_m C_m / (2a_c)] \{[(\eta_j - \eta_c) f_{Uj} f_{cj} - (\eta_i - \eta_c) f_{Ui} f_{ci}] - I_c^2 - I_c^3 + \eta_c I_c^4\} \quad (56)$$

$$C_{c6} = C_m (w_s - v_i) (f_{cj} - f_{ci}) + \left(\frac{C_m}{b}\right) (\Gamma_j f'_{cj} - \Gamma_i f'_{ci}) \quad (57)$$

$$I_c^1 = \int_{\eta_i}^{\eta_j} f_c d\eta \quad (58)$$

$$I_c^2 = \int_{\eta_i}^{\eta_j} f' f_c d\eta \quad (59)$$

$$I_c^3 = \int_{\eta_i}^{\eta_j} \eta f'_U f_c d\eta \quad (60)$$

$$I_c^4 = \int_{\eta_i}^{\eta_j} f' f'_U f_c d\eta \quad (61)$$

In the above equations, f' = derivative of the shape function with respect to η .

References

- Abbott, M. B., and Minns, A. W. (1998). *Computational hydraulics*, 2nd Ed., Brookfield Vt., Andershot, U.K.
- Abdel-Gawad, S. M., and McCorquodale, J. A. (1984). "Strip integral method applied to settling tanks." *J. Hydraul. Eng.*, 110 (1), 1–17.
- Bechteler, W., and Schrimf, W. (1984). "Improved numerical model for sedimentation." *J. Hydraul. Eng.*, 110(3), 234–246.
- Bechteler, W., and Schrimf, W. (1985). "A numerical calculation for the deposition fine sediment in horizontal settling basins." *Proc., 21st IAHR Congress*, Melbourne, Australia, 19–23.
- Bradbury, L. J. S. (1965). "The structure of a self preserving turbulent plane jet." *J. Fluid Mech.*, 23, 31–64.
- Camp, T. R. (1943). "Sedimentation and the design of settling tanks." *Trans. Am. Soc. Civ. Eng.* 2285(3), 895–936.
- Chapra, S. C., and Canale, R. P. (2002). *Numerical methods for engineers, with software and programming applications*, 4th Ed., McGraw-Hill, Boston.
- Clements, M. S. (1966). "Velocity variation in rectangular sedimentation tanks." *Proc.-Inst. Civ. Eng.*, 34, 171–200.
- Crowe, C. T., Elger, D. F., and Roberson, J. A. (2001). *Engineering fluid mechanics*, 7th Ed., Wiley, New York.
- Davidson, M. J., and Pun, K. L. (1999). "Weakly advected jets in cross-flow." *J. Hydraul. Eng.*, 125(1), 47–58.
- Dobbins, W. E. (1944). "Effect of turbulence on sedimentation." *Trans. Am. Soc. Civ. Eng.*, 2218 (109), 629–656.
- Hazen, A. (1904). "On sedimentation." *Trans. Am. Soc. Civ. Eng.*, 53, 45–71.
- Imam, E. H. (1981). "Numerical modeling of rectangular clarifiers." PhD theses, Univ. of Windsor, Windsor, Ontario, Canada.
- Kerbs, P., Stamou, A. I., Garcia-Heras, J. L., and Rodi, W. (1996). "Influence of inlet and outlet configuration on the flow in secondary clarifiers." *Water Sci. Technol.*, 34(5–6), 1–9.
- Lakehal, D., Krebs, P., Krijgsman, J., and Rodi, W. (1999). "Computing shear flow and sludge blanket in secondary clarifiers." *J. Hydraul. Eng.*, 125(3), 253–262.
- Larsen, P. (1977). "On the hydraulics of rectangular settling basins—Experimental and theoretical studies." *Rep. No. 1001*, Dept. of Water Resources Engineering, Lund, Sweden.
- Lyn, D. A., Stamou, A. I., and Rodi, W. (1992). "Density currents and shear-induced flocculation in sedimentation tanks." *J. Hydraul. Eng.*, 118(6), 849–867.
- McCorquodale, J. A. (1976). "Hydraulic study of the circular settling tanks at the West Windsor Pollution Control Plant." *Rep. Submitted to Lafontaine, Cowie, Buratto and Associates Ltd. Consulting Engineers*, Windsor, Ont., Canada.
- McCorquodale, J. A., and Khalifa, A. (1983). "Internal flow in hydraulic jump." *J. Hydraul. Eng.*, 109(5), 684–701.
- Moses, H. L. (1968). "A strip integral method for predicting the behavior of the turbulent boundary layer." *Proc., Computation of Turbulent Boundary Layers, AFOSR-IFP-Stanford Conf.*, 76–82.
- Narayanan, R. (1972). "Theoretical analysis of flow past leaf gate." *J. Hydraul. Div., Am. Soc. Civ. Eng.*, 98(6), 993–1011.
- Naser, Gh. (1993). "Flow prediction in sedimentation basins." MSc thesis, Univ. of Tarbiat-Modarres, Tehran, Iran.
- Naser, Gh., Karney, B. W., and Salehi Neishaboori, A. A. (2003). "Strip integral method application to flow prediction in sedimentation basins." *Proc., 11th Annual Conf. of CFD*, Vancouver, Canada, Vol. 1, 9–15.
- Naser, Gh., Salehi Neishaboori, A. A., and Karney, B. W. (2002). "Velocity and concentration prediction in sedimentation basins." *Proc., 1st Symp. on Envi. and Water Research Systems Analysis, EWRI Proc.*, Roanoke, Va.
- Nezu, I., and Nakagawa, H. (1993). *Turbulence in open channel flows*, Rotterdam Brookfield, Balkema, Rotterdam, the Netherlands.
- Rajaratnam, N. (1965). "Submerged hydraulic jump." *J. Hydraul. Div., Am. Soc. Civ. Eng.*, 91(4), 71–96.
- Rajaratnam, N. (1976). *Turbulent jets*, Elsevier Scientific Amsterdam, Netherlands.
- Rajaratnam, N., and Humphries, J. A. (1984). "Turbulent nonbuoyant jets." *J. Hydraul. Res.*, 22(2), 103–115.
- Rodi, W. (1980). *Turbulence models and their application in hydraulics, A state of the art review*, IAHR, Delft, The Netherlands.
- Schamber, D. R., and Larock, B. E. (1978). "A finite element model of turbulent flow in primary sedimentation basins." *Proc., Finite Element in Water Research*, FE2, London, 3.3–3.21.
- Schamber, D. R., and Larock, B. E. (1981). "Numerical analysis of flow in sedimentation basins." *J. Hydraul. Div., Am. Soc. Civ. Eng.*, 107(5), 575–591.
- Schlichting, H. (2000). *Boundary layer theory*, 8th Ed., McGraw-Hill, New York.
- Takacs, I., Patry, G. G., and Nolasco, D. (1991). "A dynamic model of the clarification-thickening process." *Water Res.*, 25(10), 1263–1271.
- Townsend, A. A. (1956). *The structure of turbulent shear flow*, Cambridge University Press, Cambridge, U.K.
- Zhou, S., and McCorquodale, J. A. (1992). "Modeling of rectangular settling tanks." *J. Hydraul. Eng.*, 118(10), 1391–1405.